Self-Trapped Excitons in Silicon Dioxide: Mechanism and Properties

Sohrab Ismail-Beigi[1] and Steven G. Louie[2]
[1]Department of Applied Physics, Yale University, New Haven, Connecticut 06520, USA
[2]Department of Physics, University of California, and Materials Sciences Division, Lawrence Berkeley National Laboratory, Berkeley, California 94720, USA

(Received 10 June 2005; published 6 October 2005)

Irradiating silica produces self-trapped excitons (STEs) that spontaneously create atomic-scale distortions on which they localize themselves. Despite enduring interest in STEs and subsequent defects in this key technological material, the trapping mechanism and geometry remain a mystery. Our *ab initio* study of STEs in α-quartz using a many-electron Green's function approach answers both questions. The STE comprises a broken O-Si bond with the hole localized on the defected oxygen and the electron on the defected silicon atom in a planar sp^2 conformation. The results further explain quantitatively the measured STE spectra.

DOI: 10.1103/PhysRevLett.95.156401 PACS numbers: 71.15.Qe, 71.35.Aa, 71.35.Cc, 71.55.Ht

Silicon dioxide is a crucial high technological material. It is the central ingredient in the metal-oxide-semiconductor (MOS) structure governing modern electronic devices and is used in optical fibers and precision frequency-control oscillators. The ever-decreasing size of electronics has pushed MOS size into the nanometer scale where the presence of atomic-level defects affects device reliability [1]. Defects in silica also degrade the performance of MOS-based electronics by creating long-lived voltage shifts [2], change dispersion and attenuation in optical fibers [3], and modify oscillator frequencies [4,5]. Many such defects are created by radiation which is problematic because SiO_2-based devices are often employed in environments subject to ionizing radiation (in satellites, nuclear power plants, medical studies, etc.) [2,4,5].

The self-trapped exciton (STE) is one of the important radiation-induced defects in silica. Excitons in silica self-trap from low to at least room temperatures [6–15]. Self-trapping occurs in an otherwise ideal structure when the excited electron and hole spontaneously create a localized distortion in the lattice which lowers their total energy and thus localizes and traps them at the distortion. The process exemplifies spontaneous symmetry breaking. The STE in α-quartz has a triplet spin state, has a long lifetime at low temperature ($\sim$ 1 ms), causes an expansion of the crystal, and has a dramatic Stokes shift of $\sim$6 eV with blue luminescent emission centered at 2.6–2.8 eV [6,7,10–15]. Creating STEs in silica leads directly to the formation of two other important defects, the E' center and the nonbridging oxygen hole center (NBOHC) [10,15]. The E' is the main candidate for the defect that determines the radiation response of MOS devices [2], and it may change the refractive index of optical fibers [3]. Therefore, a detailed theoretical understanding of the atomic-scale structure and properties of the STE will provide a step forward in understanding the physics of subsequent defect formation.

Previous theoretical studies of the STE in silica used methods based on quantum chemistry and density functional theory (DFT) of both semiempirical and *ab initio* varieties [16–20]. Cluster based quantum chemical methods are in principle highly accurate, but in practice, limitations on cluster sizes and basis sets produce sizable finite-size and convergence uncertainties [18]: at least three different configurations for the STE are found, each with its own luminescent signature [18]. DFT calculations with periodic boundary conditions and plane-wave bases do not suffer from these problems, but time-independent DFT has serious problems describing excited states: unstable trapped excitons are predicted with energies higher than perfectly delocalized ones [18,20]. In principle, time-dependent DFT (TDDFT) can describe excitations accurately, but the commonly used TDDFT exchange-correlation kernels (e.g., TDLDA) do not improve DFT's failure for the bulk [21]. New kernels are being developed with the aim of overcoming such problems, but these kernels are designed to reproduce the behavior of the Green's function methods that we utilize [22].

Here, we employ a first-principles many-electron Green's function method [23–25]. The method uses periodic supercells and naturally includes the crystalline environment, long-range screening, and relaxations. It also incorporates key electronic correlations for an accurate description of excited states and produces excellent quantitative agreement with experiments, as shown in the literature and below. Calculated excitation energies for semiconductors, insulators, or molecules are typically accurate to within 0.1–0.2 eV [23–25], which are sufficient for meaningful comparisons to experiments.

In this study, the electronic ground state is described by DFT within the local-density approximation (LDA) using the plane-wave supercell approach with norm-conserving pseudopotentials [26,27]. (The silicon pseudopotential has the $3s^2 3p^1 3d^1$ configuration with $r_c = 2.0a_0$ and oxygen $2s^2 2p^4$ with $r_c = 1.5a_0$; occupying the Si $3d$ state leads to more a transferable pseudopotential, particularly in the d channel.) The plane-wave cutoff is 70 Ry. We use an 18-atom supercell of α-quartz in the shape of a rectangular parallelepiped. We sample the Brillouin zone on a randomly shifted $2 \times 2 \times 2$ k-point grid. Predicted equilibrium lattice constants and atomic positions are within a few percent of experiment, typical of DFT-LDA.

Quasiparticle excitations are calculated by solving the Dyson equation for the one-particle Green's function within the GW approximation to the electron self-energy [23]. We fix the dielectric function to its RPA value as provided by DFT while self-consistently solving the Dyson equation within the quasiparticle approximation. We assume identical DFT and GW quasiparticle wave functions. Optically, excitations are determined by solving the Bethe-Salpeter equation (BSE) for the two-particle Green's function [24]. Our calculated excitation energies include dynamical screening [24]. All parameters are chosen to converge energy eigenvalue differences (Kohn-Sham, GW, or BSE) to 50 meV. We calculate excited-state ionic forces using our recently developed approach [25]. This allows us to find the geometrical relaxation for the excited system and thus the Stokes shift and concomitant changes of spectral properties.

Figure 1 compares the imaginary part of the frequency-dependent dielectric function for α-quartz based on the single-particle RPA-GW method (i.e., interband transitions from noninteracting electrons and holes with GW energies), solution of the BSE, and experiment. The qualitative failure of the interband method in describing the absorption onset and spectral distribution of transitions points to the overriding importance of excitonic phenomena in silica. Conversely, the GW-BSE method provides excellent quantitative predictions for the positions and amplitudes of the absorption peaks.

To describe exciton self-trapping in α-quartz, we begin with our 18-atom supercell in the ideal crystalline geometry. The ions are shifted randomly by a small amount (± 0.02 Å) to mimic inevitable thermal fluctuations that break the ideal crystalline symmetry. For the lowest-energy triplet excited state, the excited-state ionic forces are calculated, and the system is relaxed to the nearest energy minimum on the excited-state energy surface using steepest descents. We find a minimum-energy structure where one oxygen atom breaks its bond with a neighboring silicon atom which moves into a threefold coordinated planar geometry (detailed below). The configuration is the STE. As a check, the entire minimization is repeated starting with a new random initial configuration, and the same unique final structure is found.

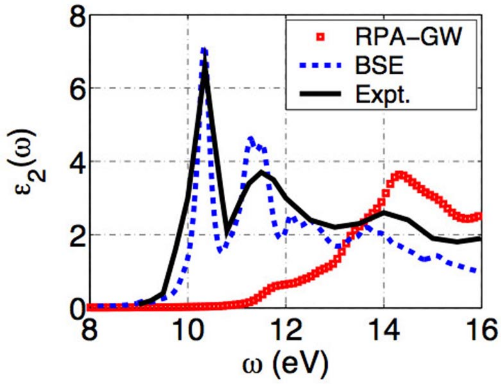

FIG. 1 (color online). Imaginary part of the frequency-dependent macroscopic dielectric function for α-quartz. Red squares are calculated results neglecting electron-hole interactions, blue dashes are calculated including electron-hole interactions, and the solid black is experimental data [32].

Figure 2 shows the calculated ground-state energy, triplet excited-state energy, and the exciton excitation energy versus the length of the ruptured Si-O bond along the relaxation pathway on the excited-state energy surface, going from the extended exciton to the STE. (These energies are functions of all the atomic positions; we are plotting them versus only one relevant degree of freedom.) The self-trapping reduces the total triplet exciton energy by roughly 2 eV, while the reduction in excitation energy, i.e., the Stokes shift, is about 6 eV. Crucially, there is no energy barrier for self-trapping.

Figure 3 displays our calculated geometry and the electron and hole probability distributions for the STE, and Table I lists key bond lengths and angles. Clearly, both the electron and hole are highly localized about the ruptured bond. Our STE contains precursors of the E′ and NBOHC centers. The hole is trapped in a $2p$ orbital of the singly coordinated oxygen atom, which is the candidate for the NBOHC [28]. The triply coordinated silicon atom assumes a planar sp^2 configuration in relation to its three remaining oxygen neighbors. The electron is localized primarily on this silicon and to a smaller extent on the three oxygens. If we remove the singly coordinated oxygen, we find the

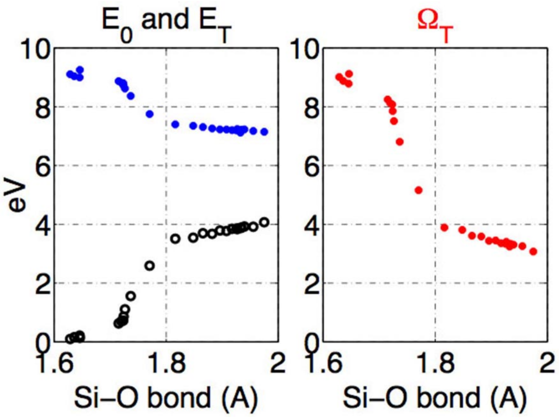

FIG. 2 (color online). Left: total ground-state energies (open circles) and triplet excited-state energies (solid dots) vs the Si-O bond length sampled along the relaxation path going from the delocalized exciton to the STE. The bond refers to the Si-O pair whose bond ruptures during formation of the STE. Right: excitation energy (or equivalently the luminescence energy at that configuration) for the triplet exciton vs the length of the ruptured bond.

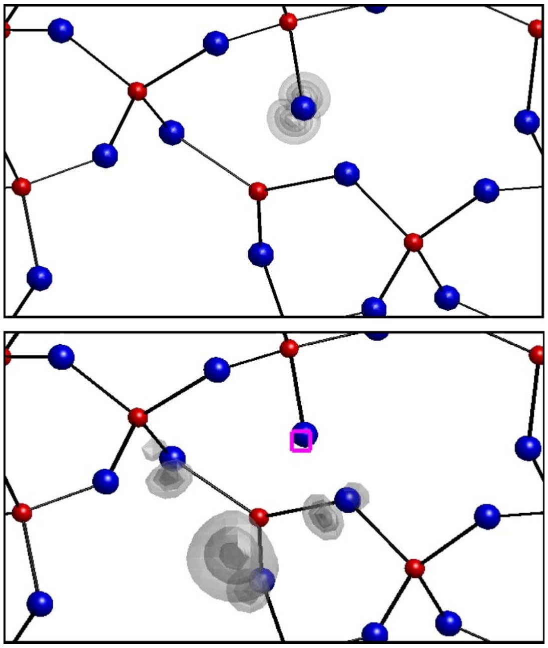

FIG. 3 (color online). Top: isosurfaces of probability for finding the hole in the self-trapped configuration. The view is along the *c* axis. Smaller red and larger blue spheres represent Si and O atoms, respectively. Bottom: isosurfaces of the conditional electron probability when the hole is located at the position indicated by the square in the self-trapped configuration. Isosurfaces are at 80%, 60%, 40%, and 20% of the maximum.

candidate for the E′ center [29]. We briefly compare these distributions and geometry to previous *ab initio* findings. In the notation of Table I, Ref. [17] found a broken Si_1-O_1 bond (2.03–2.20 Å) and a hole localized on O_1; however, it also found a shrunken Si_2-O_1 bond (1.48–1.57 Å) and, unusually, a substantial presence of the electron on O_1 (15%–30%). References [18,20] found three different STE structures, two of which ("STE-A" and "Si-dist") had a single broken Si_1-O_1 bond. STE-A, which is similar to our geometry, was stable in clusters but unstable in a bulk supercells. Si-dist had a long broken Si_1-O_1 bond (2.54–2.81 Å), and had Si_1 move substantially through the plane of O_{other} atoms to a puckered configuration, quite different from our planar arrangement; this Si_1 further backbonds with an O atom in the lattice.

TABLE I. Basic geometry of the STE. O_1 refers to the oxygen with a broken bond. Si_1 refers to the threefold coordinated silicon. Si_2 refers to the silicon to which O_1 remains bonded. O_{other} refers to the remaining three neighbors of Si_1.

Bond lengths (Å)			Bond angles (deg)		
	Bulk	STE		Bulk	STE
Si_1-O_1	1.60	1.97	O_1-Si_1-O_{other}	109	≈ 85
Si_2-O_1	1.60	1.68	O_{other}-Si_1-O_{other}	109	≈ 120
Si_1-O_{other}	1.60	1.66			

Table II presents our predicted energetic and optical emission properties for the STE. There is excellent quantitative agreement between experimental data and our *GW*-BSE results, with the expected energy accuracy of 0.1–0.2 eV. For comparison, we present results based on the constrained local spin-density approximation (CLSDA) [30]. CLSDA describes the exciton as the self-consistent solution to the DFT problem with excited electronic occupancies. The failure of the CLSDA is salient for the large Stokes shift, one of the prominent features of the STE. The CLSDA calculations are plagued by numerous other problems [18,20]. For example, self-trapping within CLSDA is prevented by an energy barrier: the tabulated CLSDA data are found by initially stretching the Si-O bond substantially (> 0.1 Å) before relaxing. If CLSDA relaxations begin with the initial geometry used in the *GW*-BSE calculations, the system reverts to the perfect crystal. We emphasize that no barrier was found in the *GW*-BSE approach where the STE forms spontaneously. These problems underline the importance of the many-electron, correlated nature of the exciton problem.

Analysis of the calculated results elucidates the mechanism for exciton self-trapping. The low-lying unoccupied bands in quartz arise from antibonding Si-O states. Exciting an electron into them weakens the Si-O bond and makes its rupture possible. The exciton can reduce its energy by distorting the lattice so as to lower the energy of the electron-occupied state and raise the energy of the unoccupied state. These energy shifts generate the Stokes shift. The energy reduction from the electronic levels competes with the loss of bonding/cohesive energy from the structural distortion. In a molecular system, all electronic states are spatially confined, and the excited system should always distort because the energy lowering from the level shifts is linear in the distortion amplitude while the cohesive energy penalty is quadratic.

The situation in crystals differs from molecules in an important respect concerning confinement. Excitons are two-particle states, and their wave functions may be described using the center of mass coordinate and the electron-hole relative or separation coordinate. In undistorted crystals, Bloch's theorem obliges the center of mass to have a well-defined crystal momentum and hence be completely delocalized. For tightly bound excitons, the

TABLE II. STE properties from experiments, *GW*-BSE calculations, and CLSDA calculations: Ω_T, luminescent emission energy; ΔE_{Stokes}, Stokes shift; *P*, degree of polarization of emitted light along the *c* axis. Experimental ranges indicate lowest and highest values found in the references.

Method	Ω_T (eV)	ΔE_{Stokes} (eV)	*P*
Experiment [6,10–14]	2.6–2.8	6.2–6.4	0.48–0.70
GW-BSE	2.85	6.37	0.72
CLSDA	4.12	2.14	⋯

relative coordinate is confined to a few bond lengths. For weaker binding characteristic of many semiconductors, the range is 10–100 bond lengths. For self-trapping to occur, both coordinates must become confined about the distortion site with an extent of at most a few bond lengths (exemplified in Fig. 3). Both confinement effects cost kinetic energy and oppose self-trapping.

The properties of silica favor exciton self-trapping. We find that, because of strong electron-hole attraction, the untrapped exciton is already well confined in the relative coordinate whose distribution is comparable to that of the STE. For example, the electron-hole attraction energies for these two different configurations differ by only ~0.1 eV. Thus, self-trapping will not cost significant confinement energy for the relative coordinate. The confinement cost arises predominantly from the center of mass degree of freedom. Simple physical arguments [30] then show that the lowest-energy state of the excited system is either completely unconfined or highly confined to atomic dimensions. Which case prevails depends on the balance between the energy benefit from structural distortion and the confinement cost.

In SiO_2, the center of mass has a large effective mass dominated by the massive holes at the valence band edge: $m^* = (5\text{–}10)m_e$ (m_e is the free electron mass) [31]. Confining this mass in a region of a few Ångstroms costs only ~0.5 eV, small compared to electronic energy gains of ~2–5 eV. This situation differs from that of standard semiconductors such as Si, Ge, or GaAs which have (a) small effective masses $m^* \sim 0.5m_e$ and (b) untrapped excitons that are not well confined in the relative coordinate. This doubly large confinement cost explains why STEs are not observed readily in these semiconductors.

In summary, we investigated the STE in α-quartz using state-of-the-art *ab initio* many-electron Green's function methods. Our results show that the STE forms by breaking a Si-O bond, substantially distorting the surrounding atomic structure and localizing on this distortion. The excited electron and hole are localized on the broken-bond Si and O atoms, respectively. Our predicted properties for the STE are in excellent quantitative agreement with experiments. The theoretical results illuminate the relevant physics of the trapping mechanism and underline aspects unique to crystalline systems.

This work was supported by NSF Grant No. DMR04-39768 and by the Office of Energy Research U.S. DOE Contract No. DE-AC03-76SF00098. Computer resources were provided by the DOE at the LBNL NERSC and by the NSF NPACI at the SDSC. This work was facilitated by the DOE Computational Materials Science Network.

---

[1] G. D. Wilk, R. M. Wallace, and J. M. Anthony, J. Appl. Phys. **89**, 5243 (2001).
[2] F. B. McLean, H. E. Boesch, Jr., and T. R. Oldham, *Ionizing Radiation Effects in MOS Devices and Circuits*, edited by T. P. Ma and P. V. Dressendorfer (Wiley, New York, 1989), Chap. 3.
[3] A. Othonos, Rev. Sci. Instrum. **68**, 4309 (1997).
[4] P. Pellegrini *et al.*, IEEE Trans. Nucl. Sci. **NS-25**, 1267 (1978).
[5] L. E. Halliburton *et al.*, IEEE Trans. Nucl. Sci. **NS-26**, 4851 (1979).
[6] W. Hayes *et al.*, J. Phys. C **17**, 2943 (1984).
[7] M. A. Stevens Kalceff and M. R. Phillips, Phys. Rev. B **52**, 3122 (1995).
[8] D. L. Griscom, *Proceedings of the Thirty-Third Frequency Control Symposium* (Electronic Industries Association, Washington, DC, 1979), p. 98.
[9] L. W. Hobbs and M. R. Pascucci, J. Phys. (Paris), Colloq. **41**, C6-237 (1980).
[10] G. Guizard *et al.*, J. Phys. Condens. Matter **8**, 1281 (1996).
[11] K. Tanimura, T. Tanaka, and N. Itoh, Phys. Rev. Lett. **51**, 423 (1983).
[12] K. Tanimura and L. E. Halliburton, Phys. Rev. B **34**, 2933 (1986).
[13] C. Itoh, K. Tanimura, and N. Itoh, J. Phys. C **21**, 4693 (1988).
[14] W. Joonsen *et al.*, Appl. Phys. Lett. **61**, 2260 (1992).
[15] P. N. Saeta and B. I. Greene, Phys. Rev. Lett. **70**, 3588 (1993).
[16] A. L. Shluger, J. Phys. C **21**, L431 (1988).
[17] A. J. Fisher, W. Hayes, and M. A. Stoneham, J. Phys. Condens. Matter **2**, 6707 (1990).
[18] R. M. Van Ginhoven *et al.*, J. Chem. Phys. **118**, 6582 (2003).
[19] A. Shluger and E. Stefanovich, Phys. Rev. B **42**, 9664 (1990).
[20] J. Song, H. Jönsson, and L. R. Corrales, Nucl. Instrum. Methods Phys. Res., Sect. B **166**, 451 (2000).
[21] G. Onida, L. Reining, and A. Rubio, Rev. Mod. Phys. **74**, 601 (2002).
[22] L. Reining, V. Olevano, A. Rubio, and G. Onida, Phys. Rev. Lett. **88**, 066404 (2002); F. Sottile, V. Olevano, and L. Reining, Phys. Rev. Lett. **91**, 056402 (2003); A. Marini, R. Del Sole, and A. Rubio, Phys. Rev. Lett. **91**, 256402 (2003).
[23] M. S. Hybertsen and S. G. Louie, Phys. Rev. B **34**, 5390 (1986).
[24] M. Rohlfing and S. G. Louie, Phys. Rev. B **62**, 4927 (2000).
[25] S. Ismail-Beigi and S. G. Louie, Phys. Rev. Lett. **90**, 076401 (2003).
[26] M. C. Payne, M. P. Teter, D. C. Allan, T. A. Arias, and J. D. Joannopoulos, Rev. Mod. Phys. **64**, 1045 (1992).
[27] L. Kleinman and D. M. Bylander, Phys. Rev. Lett. **48**, 1425 (1982).
[28] L. Skuja, J. Non-Cryst. Solids **179**, 51 (1994).
[29] M. Boero, A. Pasquarello, J. Sarnthein, and R. Car, Phys. Rev. Lett. **78**, 887 (1997).
[30] F. Mauri and R. Car, Phys. Rev. Lett. **75**, 3166 (1995).
[31] J. R. Chelikowsky and M. Schlüter, Phys. Rev. B **15**, 4020 (1977).
[32] H. R. Philipp, Solid State Commun. **4**, 73 (1966).